Experimental determination of ΔH_f^0(HOBr) and ionization potentials (HOBr): Implications for corresponding properties of HOI

B. Ruscic and J. Berkowitz
Chemistry Division, Argonne National Laboratory, Argonne, Illinois 60439

(Received 14 June 1994; accepted 13 July 1994)

The photoion yield curves of $HOBr^+$ and Br^+ from HOBr are presented. The adiabatic I.P. of HOBr is found to be 10.638±0.003 eV. Autoionizing structure in $HOBr^+$ is tentatively assigned and leads to an adiabatic I.P. of the first excited ($A\ L^2\ A'$) state of ~11.46 eV. The 0 K threshold of Br^+ from HOBr (13.915±0.018 eV) implies D_0(HO–Br)≤2.101±0.018 eV≡48.45±0.42 kcal/mol. Together with auxiliary thermochemistry, this value yields $\Delta H^0_{f_{298}}$(HOBr) ≥ −13.43 ± 0.42 kcal/mol, in excellent agreement with a recent *ab initio* value −14.2±1.6 kcal/mol. The resulting proton affinity of BrO is 163.8 kcal/mol. Trends observed in the properties of OX and HOX (X=F, Cl, Br) are utilized to infer new values for ΔH^0_f(OI) and ΔH^0_f (HOI). Predictions are made for I.P.(HOI). Proton affinities of OX are seen to increase with heavier X, while the $X\ ^2A''$–$A\ ^2A'$ splitting decreases.

I. INTRODUCTION

One of the cycles which is believed to contribute to ozone destruction in the stratosphere is[1,2]

$$\begin{aligned} &Br+O_3 \rightarrow BrO+O_2, && (1)\\ &BrO+HO_2 \rightarrow HOBr+O_2, && (2)\\ &HOBr+h\nu \rightarrow OH+Br, && (3)\\ &OH+O_3 \rightarrow HO_2+O_2, && (4)\\ \text{net:}\quad &2O_3 \rightarrow 3O_2. \end{aligned}$$

As first introduced by Yung *et al.*,[1] this cycle was believed to be relatively unimportant unless reaction (2) had a rate constant "$\geqslant 4\times10^{-12}$ $cm^3\ s^{-1}$, an unlikely possibility." Recent measurements[2,3] have found $k_2=(3.4\pm1.0)\times10^{-11}$ cm^3 $molecule^{-1}$ s^{-1}, with a resulting increase in ozone depletion from this cycle, according to the model used.[2] The rate of photolysis [reaction (3)] is, to the best of our knowledge, still not known.

An additional role has recently been suggested[4] for tropospheric HOBr. In this model, HOBr is dissolved in sulfuric acid aerosols, forming aqueous Br_2, which volatilizes and is photolyzed by reaction (3), thereby contributing to ozone depletion at ground level.

Although it is the rates of the various reactions which enter the modeling (rather than the thermochemistry), Bridier *et al.*[3] have drawn attention to the correlation of rate constants with the exothermicity of the reaction for the series

$$XO+HO_2 \rightarrow HOX+O_2, \quad X=Cl,Br,I. \qquad (2')$$

In this sequence, they found that the rate constant increased from 0.5 to 3.4 to about 7 ($\times10^{-11}$ cm^3 $molecule^{-1}$ s^{-1}) for X=Cl, Br, and I, while the exothermicity varied from −46 to −52 to −65 kcal/mol (at 298 K). Although Bridier *et al.*[3] did not state the sources of their thermochemical values, it is possible to reconstruct $\Delta H^0_{f_{298}}$(ClO)=24.4, $\Delta H^0_{f_{298}}$(HOCl)=−19, $\Delta H^0_{f_{298}}$(BrO)=30.1, $\Delta H^0_{f_{298}}$(HOBr)=−19, $\Delta H^0_{f_{298}}$(IO)=41, and $\Delta H^0_{f_{298}}$(HOI)=−21, all in kcal/mol. The values for ClO and HOCl appear to be firmly established. Those for IO and HOI are poorly known. Of particular interest for the present investigation is the value chosen for HOBr. It is essentially an estimate of Benson's,[5] which has been maintained in two recent compilations[6,7] used for stratospheric modeling. It differs from two recently reported values -9^{+1}_{-4} (Ref. 8) and −14.2±1.6 kcal/mol.[9] Had Bridier *et al.* used either of these later values, their correlation of rate constants with exothermicity would be much less convincing.

Both of the recently reported values are based on *ab initio* calculations. McGrath and Rowland[9] used *G2* theory, and some semiempirical corrections, supplemented by spin–orbit corrections, to arrive at their $\Delta H^0_{f_{298}}$(HOBr), while Monks *et al.*[8] calculated the proton affinity (P.A.) of BrO and combined this information with an experimental ionization potential of HOBr to infer $\Delta H^0_{f_{298}}$(HOBr). Their calculation of P.A.(BrO) appeared to proceed by successive approximation. After learning that $\Delta H^0_{f_{298}}$(HOBr)≤−9 kcal/mol, based on the rapid reaction

$$OH+Br_2 \rightarrow HOBr+Br \qquad (5)$$

(*vide infra*), they found that the first order configuration interaction (FOCI) calculation of P.A.(BrO) was insufficient ($\Delta H^0_{f_{298}}=-2$), and finally extended the calculation to the second order multiconfiguration interaction level (SOCI) to arrive at $\Delta H^0_{f_{298}}$(HOBr)=−9 kcal/mol, which matched the allowed upper limit. The intermediate value of −2 kcal/mol was used in a contemporary publication by Monks *et al.*[10]

Still lacking is a purely experimental determination of ΔH^0_f(HOBr), which is the subject of the present research.

II. EXPERIMENTAL APPROACH

The approach we shall utilize here to infer ΔH^0_f(HOBr) is to measure the appearance potential of known fragments which, together with the corresponding I.P. of the ionic fragment, establishes an upper limit to that particular bond energy, and a lower limit to the stability of HOBr. There are three possible pairs of fragments.

(1) Br^++OH, Br+OH^+;

(2) BrO^++H, BrO+H^+;

 0021-9606/94/101(9)/7795/9/$6.00

(3) $O^+ + HBr$, $O + HBr^+$.

In each pair, the species with the lower I.P. is favored, a phenomenon sometimes called Stevenson's rule. Hence, the choices are reduced to Br^+, BrO^+, and HBr^+. Of these, the lowest energy process, based on known heats of formation, is that forming Br^+. It is also a simple bond cleavage, whereas HBr^+ involves a constrained transition state. The process forming BrO^+ introduces some ambiguity because somewhat different ionization potentials have been reported[11,12] for BrO. In fact, we examined the onset of BrO^+ in this experiment and found that its appearance potential (A.P.) was much lower than anticipated, and very likely attributable to Br_2O as progenitor (Br_2O^+ having been observed in the mass spectrum).

Hence, the focus of the investigation was the appearance potential of Br^+ from HOBr. Our method of preparation concomitantly generates some Br_2. The appearance potential of Br^+ from Br_2 at 0 K (from well-established thermochemical data) is 13.784 eV≡899.46 Å. (There are still lower energy processes due to ion-pair formation, but these are weak and distinguishable.) This appearance potential is in the region expected for Br^+ from HOBr. Therefore, it is important to minimize the abundance of Br_2 relative to HOBr in the preparation of the sample and to correct adequately for the contribution of Br_2 to the observed Br^+ signal.

Monks *et al.*[8] generated HOBr in a flow tube reactor, according to reaction (5). This approach was certain to provide us with a large abundance of Br_2 and Br, both of which would confuse our appearance potential measurements. We opted instead (initially) for a method utilized by Koga *et al.*[13] who obtained the microwave spectrum of HOBr. These authors produced HOBr by reacting an excess of liquid bromine with a slurry of HgO in water. The sample was degassed, excess bromine was removed by pumping, and the gaseous sample (kept at −20 °C) was introduced into the apparatus. We had moderate success with this method, and somewhat better success by stirring water and bromine in an ice bath, and adding HgO slowly. Our best preparation, both in terms of the HOBr:Br_2 ratio and in the absolute abundance of HOBr, was achieved by stirring an excess of water with bromine in an ice bath, and then adding Ag_2O powder. The vessel was loosely sealed and stirred for about 2 h, during which time the solution became orange, then pale yellow. The pale yellow liquid was decanted and placed in a vessel maintained at −20 °C. Under these conditions, the $HOBr^+$ intensity was approximately five times that of Br_2^+ at 800 Å. Since the fragmentation ratio (Br^+:Br_2^+) is about 1:10, while that of Br^+:$HOBr^+$ was found to be ~1:4.5, the contribution of Br_2 to the Br^+ signal was ≲10% throughout most of the region of interest. This contribution was subtracted from the measured Br^+ signal by establishing the photoion yield curve of Br^+ from Br_2 in a separate experiment, and then utilizing this function with a measured Br_2^+ abundance to determine the quantity to be subtracted.

The photoionization mass spectrometric apparatus, previously described,[14] consists of a 3 m vacuum ultraviolet monochromator and a quadrupole mass spectrometer. The hydrogen many-line emission spectrum was utilized as a light source in reexamining the parent ionization of HOBr in the lower energy region, while the helium Hopfield continuum was employed to measure Br^+ and $HOBr^+$ at higher energies. The wavelength resolution was 0.83 Å full width at half-maximum (FWHM). Calibration wavelengths in the hydrogen region included atomic Lyman α, β, and well-known molecular emission bands. In the helium region, various impurity emission lines served as calibrants.

III. EXPERIMENTAL RESULTS

Figure 1 is an overview of the photoionization of HOBr between 800 Å and the ionization threshold, displaying

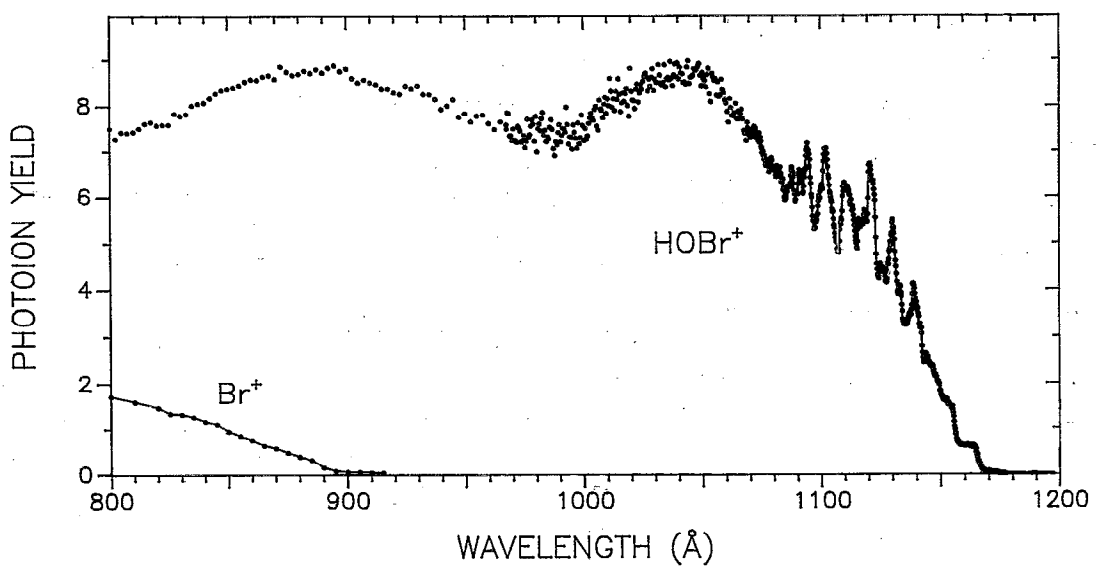

FIG. 1. An overview of the photoion yield curves of $HOBr^+$ and Br^+ from HOBr between 800 Å and the ionization threshold. The relative abundance of Br^+ and $HOBr^+$ is correctly depicted in the figure, apart from quadrupole transmission factors.

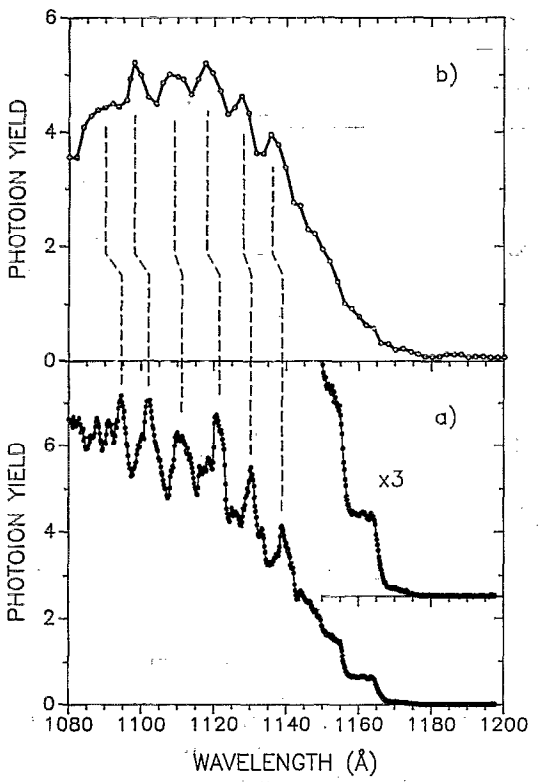

FIG. 2. (a) Expanded curve of $HOBr^+$ from HOBr between 1080–1190 Å (present data). (b) The same region as in (a) taken from Ref. 8. The jogged dotted lines indicate the mismatch of the peaks in the two data sets. The threshold region is shown further enlarged in the inset.

$HOBr^+$ and Br^+ with the correct relative abundance (apart from small quadrupole transmission factors). The parent ion displays a sharp step structure near threshold (unlike the sloping onset in Ref. 8), then a region of autoionizing structure (*vide infra*), followed by a broad band. The Br^+ fragment increases monotonically and nearly linearly from its threshold.

A. Detailed examination of $HOBr^+$ from HOBr

1. The threshold region

Figure 2(a) is an expanded curve of the parent ion in the region of autoionizing structure, extending to below the threshold. Figure 2(b) taken from the recent publication of Monks *et al.*[8] displays the same region. In Fig. 2(a), the wavelength resolution is 0.83 Å, and points are taken at 0.20 Å intervals, while in Fig. 2(b), the stated spectral width is 2.3 Å, and the spacing between points is 1.0 Å. Apart from the resolution, another marked difference between the spectra is the location of the peak positions. The data of Monks *et al.* appear to shorter wavelength than the present data by ~2.2–4.4 Å, averaging about 3.5 Å. Below ~1100 Å, their ion yield curve declines rapidly, missing the last sequence of peaks. This behavior is likely attributable to the transmission cutoff of the LiF window used in their experiment. We have examined the peak region ~1120 Å at much higher resolution (0.14 Å, FWHM), and found little or no evidence for further splitting. Hence, we believe that the spectrum shown in Fig. 2(a) displays inherent, rather than instrumentally limited width. Monks *et al.* were unable to assign the autoionizing structure. We defer discussion of this structure to the following section.

In Fig. 2(a), step-like structure can be seen in the threshold region between ~1150–1165 Å. This region is further amplified in the inset to Fig. 2. The idealized threshold behavior for photoionization is just such a step function. The curvature at the ascent is very likely due to rotational effects, while the spacing between steps corresponds to a vibrational quantum in the electronic ground state of $HOBr^+$. This spacing is about 0.089 ± 0.004 eV$\equiv720\pm30$ cm^{-1}. The O–Br stretching frequency in neutral HOBr (Ref. 15 and 16) is very nearly 620 cm^{-1}. If this step in $HOBr^+$ is identified with the O–Br stretching frequency in the cation, it corresponds to a 16% increase from the value in HOBr, implying that this first ionization energy involves removal of an electron from an antibonding orbital. The halogen and interhalogen molecules, although having $D_{\infty h}$ and $C_{\infty v}$ symmetries, provide useful comparisons. In each instance, these molecules have π_g-like uppermost occupied orbitals, which are antibonding. The molecule ClBr comes closest to approximating HOBr, since the ionization potential of Cl is close to that of OH. Dunlavey *et al.*[17] have obtained the partial He I photoelectron spectrum of ClBr. They observed the spin–orbit split $^2\Pi_{3/2}$ and $^2\Pi_{1/2}$ states, each with its vibrational progression. The increase in vibrational frequency from $ClBr^+$ was found to be 9% for $^2\Pi_{3/2}$ and 14% for $^2\Pi_{1/2}$, similar to that found here for HOBr. Four vibrational peaks could be seen for $^2\Pi_{3/2}$, the second ($v'=1$) being the largest. In an idealized photoionization spectrum, the step height is proportional to the Franck–Condon factor. In the present spectrum [Fig. 2(a)], the height of the second step is seen to be larger than the first or third.

In the He I photoelectron spectra of HOF (Ref. 18) and HOCl,[19] four or five members of a vibrational progression are seen near threshold, with the second peak being the largest.

It seems clear that the threshold region of $HOBr^+$(HOBr) manifests vibrational steps with rotational tailing. In principle, it is possible[20] to fit the rotational tail, by superposing the various rotational transitions, and selecting what would be the Q branch. Here, we approximate this solution by choosing the half-rise point of the first step 1165.5 ± 0.3 Å$\equiv10.638\pm0.003$ eV. Monks *et al.*[8] deduced $10.61_7\pm0.03_6$ eV, not too different from the present value. However, it seems to be due to a cancellation of errors. We have already noted that their wavelength scale appears to be off by ~3.5 Å, in a direction which would yield a higher ionization threshold. Their method of arriving at an adiabatic ionization potential is to linearly extrapolate a sloping threshold, which we found to be a step. There is no obvious justification for such an extrapolation, which they extended to their zero background base line. This procedure has the effect of lowering the apparent ionization potential. Thus, the two errors approximately compensate one another.

2. The region of autoionization structure

Figure 3 focuses on the autoionizing region. As mentioned earlier, improved instrumental resolution is not likely

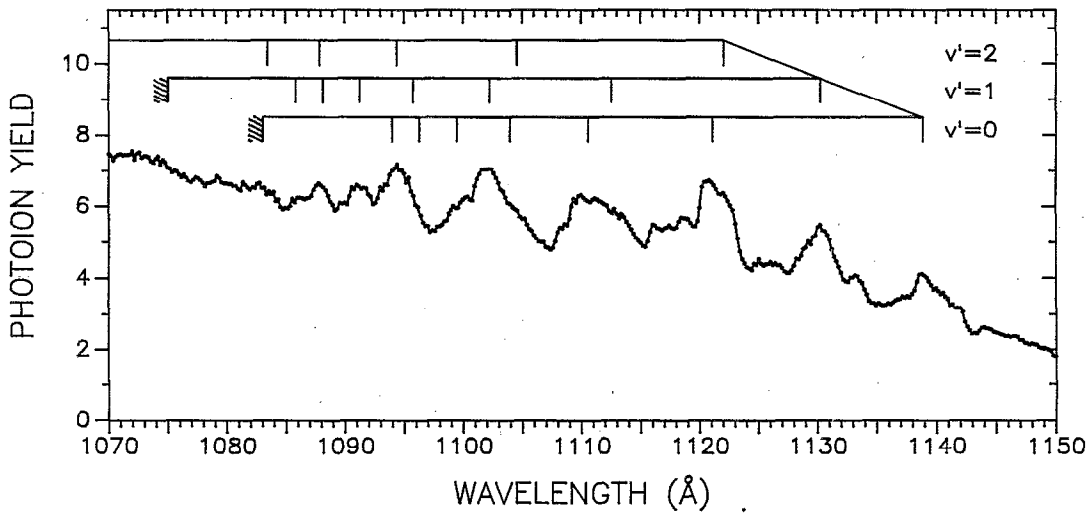

FIG. 3. The autoionizing region of the photoion yield curve of $HOBr^+$ (HOBr), with tentative assignments shown in the diagram surmounting the figure.

to simplify this spectrum. A plausible assignment of this structure, which rationalizes the major features, appears in the upper half of Fig. 3. The fit is not perfect, but perhaps this cannot be expected without inclusion of perturbations in such a congested spectrum. The attractiveness of the assignment is its simplicity. It consists of a single Rydberg series, each member of which has a progression of four (or more) vibrational states. A single quantum defect $\delta = n - n^* \cong 1.1$ is used to characterize this series, taken to be an *nd* series.

Two consequences of this assignment are that the adiabatic I.P. is ~11.46 eV and the vibrational frequency is about 0.083 eV≡670 cm^{-1}. This implies an excitation of ~6600 cm^{-1} for the limiting ion state above the ground state.

Monks *et al.*[8] have calculated 6631 cm^{-1} for an A' state above the ground $^2A''$ state, but appeared to discount Rydberg states converging to this limit because such transitions are "essentially two electron in nature, the transition probability is low, and the Rydberg states of the A state should not contribute significantly to the ionization." Support for the present interpretation comes from the He I PES of HOCl,[19] where this first excited state is observed, assigned to the A' state, and found to be of comparable intensity to the ground state.

Weaker structure appearing in Fig. 3 is due probably to one or more additional Rydberg series converging to the same limits of the A' state.

B. Br^+ from HOBr

A magnified view of the photoion yield curve of Br^+ is presented in Fig. 4. The experimental data prior to subtraction (representing Br^+ from a mixture of Br_2 and HOBr) and after subtraction of $Br^+(Br_2)$ are shown. A linear kernel function, convoluted with a thermal broadening function fitted to the latter data (see the Appendix) yields a 0 K threshold of 13.915±0.018 eV. The vibrational frequencies of HOBr used to calculate the vibrational contribution to the offset were 3589, 1162.3, and 619.5 cm^{-1}. The two latter frequencies were taken from McRae and Cohen[15] and the first from Schwager and Arkell.[16] Almost the same frequencies have been mentioned by Barnes *et al.*[21,22] Together, they account for only 0.106 kcal/mol, whereas rotations contribute 0.889 kcal/mol to the internal thermal energy.

Upon subtracting the value[23] of the ionization potential of Br (11.8138 eV) from the above appearance potential, one obtains $D_0(HO-Br) \leqslant 2.101 \pm 0.018$ eV, or 48.45±0.42 kcal/mol, which is a rigorous upper limit to this quantity. Since the dissociative ionization process measured is the lowest energy one, and involves a simple bond scission, it is plausible to assume that this upper limit is very close to the true value.

IV. INTERPRETATION OF RESULTS

A. The heat of formation of HOBr

In Sec. III B, we obtained $\Delta H_0 \leqslant 48.45 \pm 0.42$ kcal/mol for the reaction

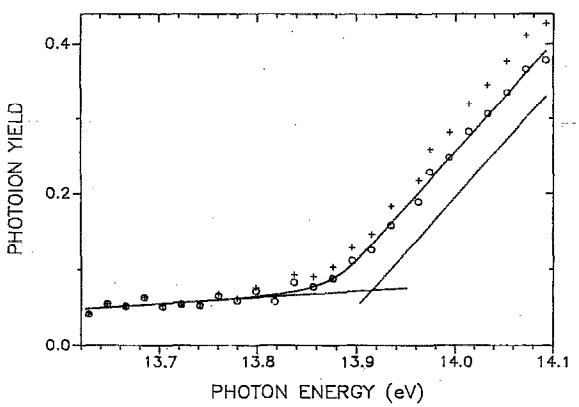

FIG. 4. Photoion yield curve of Br^+ from HOBr. The upper curve (crosses) consists of Br^+ from a mixture of HOBr and ~10% Br_2. In the lower curve (circles), the contribution of Br^+ from Br_2 has been subtracted. The smooth curve drawn through the points is the best fit of a linear kernel function, convoluted with a thermal broadening function (see the Appendix). The sloping line to higher energy is the hypothetical 0 K kernel function.

HOBr→Br+OH.

With $\Delta H_{f_0}^0$(OH)=9.34±0.05 kcal/mol, (Ref. 24) and $\Delta H_{f_0}^0$(Br)=28.18±0.03 kcal/mol, we compute $\Delta H_{f_0}^0$(HOBr) ≥−10.93±0.42 kcal/mol and $\Delta H_{f_{298}}^0$(HOBr)≥−13.43 ±0.42 kcal/mol. This experimental result is in excellent agreement with the recently reported[9] calculated value, $\Delta H_{f_{298}}^0$(HOBr)=−14.2 ± 1.6 kcal/mol, considering that this molecule contains a third row atom.

Boodaghians *et al.*[25] studied the temperature dependence of reaction (5) (see the Introduction) and found zero activation energy (E_a), at the 95% confidence limit, with a "maximum value of E_a that can be accommodated" of 1.3 kcal/mol. With $\Delta H_{f_{298}}^0$ values for OH, Br, and Br_2 taken from Gurvich *et al.*,[24] and the currently deduced $\Delta H_{f_{298}}^0$(HOBr), we find that reaction (5) is exothermic by 3.48±0.42 kcal/mol.

V. DISCUSSION

A. Implications for ΔH_f^0(IO) and ΔH_f^0(HOI)

In the Introduction, we noted that Bridier *et al.*[3] had found an apparent correlation between the exothermicities of the reactions (2′) and the corresponding reaction rates. With our current value for $\Delta H_{f_{298}}^0$(HOBr), the exothermicities of the ClO+HO_2 and BrO+HO_2 reactions are virtually identical, although the rates differ by a factor of 6–7.

The heats of formation of XO and HOX (X=F, Cl, Br) now seem to be fairly well established, but the corresponding values of IO and HOI are wildly discordant. In a recent study of the reaction of IO with HO_2, presumably forming HOI+O_2 [one of the variants of reaction (2′)], Maguin *et al.*[26] attempted to evaluate the exothermicity of that reaction. They noted wide variations in $\Delta H_{f_{298}}^0$(IO), but chose 41.1 kcal/mol. For $\Delta H_{f_{298}}^0$(HOI), they accepted the limits −18.4 to −24.4 kcal/mol inferred by Jenkin *et al.*[27] and used −21.4±3.0 kcal/mol. In Table I, we compare the HO–X bond energies and the O–X bond energies to explore some systematic behavior, temporarily using the heats of formation of IO and HOI employed by Maguin *et al.* In Table II, a similar comparison is made for the H–OX bond energies.

In Table I, one notes an increase in both HO–X and O–X bond energies between X=F and Cl, then a decrease in both between Cl and Br. The ratio D_0(HO–X):D_0(O–X) may decline slightly from 0.92±0.04 to 0.875±0.0015. However, between Br and I, D_0(HO–X) increases, while D_0(O–X) decreases markedly, and the ratio becomes 1.36. This comparison suggests that some reexamination of the values of ΔH_f^0(HOI) and ΔH_f^0(IO) is in order. In Table II, the H–OX bond energies vary from 97.1 to 93.8 to 94.2 kcal/mol in the sequence HOF–HOCl–HOBr; with H–OI, there is a marked increase to 114 kcal/mol. This comparison also invites some reinvestigation.

Let us first examine ΔH_f^0(IO). A value of $\Delta H_{f_{298}}^0$(IO) = 41.1 kcal/mol [$\Delta H_{f_0}^0$(IO) = 41.6 kcal/mol] implies D_0(IO)=43 kcal/mol≡1.86 eV. Huber and Herzberg[28] examined alternative Birge–Sponer extrapolations and chose D_0(IO)=1.8 eV. Earlier, Gaydon[29] (with largely similar sources of information) arrived at D_0(IO)=2.0±0.2 eV≡46±5 kcal/mol. Huber and Herzberg appeared to have overlooked, or discounted, a molecular beam study of the reaction

O+ICl→IO+Cl

by Radlein *et al.*,[30] from which these authors deduced D_0(IO)=53±3 kcal/mol. This is the value adopted in the later compilation by Gurvich *et al.*[24] A more recent attempt at fitting five vibrational levels of the ground state of IO by Reddy *et al.*[31] gives D_0(IO)=2.543±0.013 eV ≡58.64±0.30 kcal/mol, but concomitant work by these authors on D_0(ClO) using ten vibrational levels is too high by ~0.2 eV, and hence does not lend confidence to their IO result. We tentatively choose D_0(IO)=50±5 kcal/mol, roughly the mean of the preferred values of Radlein *et al.* and Gaydon, and within their respective error limits.

Jenkin *et al.*[27] arrived at an upper limit for $\Delta H_{f_{298}}^0$(HOI) by noting that the reaction of OH with CF_3I occurs rapidly. That reaction had been studied earlier by Garraway and Donovan,[32] who found a reaction rate of $(1.2\pm0.2)\times10^{-13}$ cm^3 $molecule^{-1}$ s^{-1}, which is not very

TABLE I. HO–X and O–X bond energies (in kcal/mol at 0 K).

X	D_0(HO–X)	D_0(X–O)	Ratio, D_0(HO–X)/D_0(XO)
F	47.3[a]	51.5±2.4[b]	0.92±0.04
Cl	55.1[c]	63.43[b]	0.86_9
Br	48.45±0.42[d]	55.3±0.6[b]	0.86–0.89
I	56.3[e]	41.5[e]	1.36
	(43)[f]	(50)[f]	(0.86)
	(44)		(0.88)

[a]In their photoionization study of HOF, Berkowitz *et al.* (Ref. 39) observed a threshold for OH^+ at 15.07 eV (0 K). At that time, the ionization potential of OH was not well established. Recently, Wiedmannn *et al.* [R. T. Wiedmann, R. G. Tonkyn, M. G. White, K. Wang, and V. McKoy, J. Chem. Phys. **97**, 768 (1922)] obtained I.P.(OH)=13.0170±0.0002 eV. These combined results yield D_0(HO–F)=2.05$_3$ eV≡47.3 kcal/mol, and consequently, $\Delta H_{f_0}^0$(HOF) = −19.5 kcal/mol. J. A. Pople and L. A. Curtiss [J. Chem. Phys. **90**, 2833 (1989)] have calculated D_0(HO–F)=48.4 kcal/mol.
[b]Reference 23.
[c]From $\Delta H_{f_0}^0$(HOCl) = −17.18 ± 0.07 kcal/mol. See Ref. 9, and also C. E. Ennis and J. W. Birks, J. Phys. Chem. **89**, 186 (1985).
[d]Present results.
[e]Values adopted by Maguin *et al.* (Ref. 26).
[f]Values suggested in this work.

TABLE II. O–H bond energies in HOX (in kcal/mol at 0 K).

H–OF	97.0±2.4[a]
H–OCl	93.0[b]
H–OBr	94.2[c]
H–OI	114[d]
	(94.2–95.2)[e]

[a]From $\Delta H_{f_0}^0$(HOF) = −19.5 kcal/mol; see footnote a of Table I.
[b]Derived from $\Delta H_{f_0}^0$(HOCl) = −17.18 ± 0.07 kcal/mol; see footnote c of Table I.
[c]Present results.
[d]Values adopted by Maguin *et al.* (Ref. 26).
[e]Values suggested in this work.

rapid. These authors monitored the OH concentration and assumed that the reaction proceeded to form $HOI+CF_3$, although the products were not measured. Their assumption was based on the presumed parallelism of halogen atom and OH reactions. Jenkin *et al.* also adopted this reaction pathway "since C–F bonds are too strong to be reactive at room temperature." Thus, taking ~53.3 kcal/mol as the C–I bond strength, they assumed that the O–I bond strength in HOI must be at least as large, and thereby deduced $\Delta H^0_{f_{298}}(HOI) < -18.4$ kcal/mol. However, another set of products could be CF_3O+HI. Even within the current range of uncertainty of $\Delta H^0_{f_{298}}(CF_3O)$, i.e., between −150 (Ref. 33) and −157 kcal/mol,[34] this reaction is at least 16 kcal/mol more exothermic than one just exothermic enough to yield $HOI+CF_3$. Consequently, until the reaction products of $OH+CF_3I$ are established, the upper limit to $\Delta H^0_f(HOI)$ fixed by Jenkin *et al.* must be regarded as questionable. Hence, any value >−24.4 kcal/mol [their derived lower limit for $\Delta H^0_{f_{298}}(HOI)$] would appear possible.

If we extrapolate the trend in the ratio $D_0(HO-X):D_0(O-X)$ in Table I, we estimate this ratio to be 0.86–0.88 for X=I. This, in turn, gives $D_0(HO-I)=43-44$ kcal/mol and $\Delta H^0_{f_0}(HOI)=-8$ to −9 kcal/mol. With this value, $D_0(H-OI)$ in Table II becomes 94.2–95.2 kcal/mol, which is essentially the value for $D_0(H-OBr)$ and $D_0(H-OCl)$. These suggested values in Tables I and II are given in parentheses.

What evidence can be offered in support of these suggested values? While internuclear distances and vibrational frequencies are not reliable guides to dissociation energies, they provide some indications. The molecular structures of HOF, HOCl, and HOBr are known,[13,35] but that of HOI is not. The OH distances in these molecules are 0.964±0.01, 0.975±0.003, and 0.961±0.001 Å, in the order given. Insofar as they can be correlated with bond energies, they imply roughly constant values, as is observed. It seems unlikely to us that the H–OI bond energy will increase dramatically (by ~20 kcal/mol) from the other H–OX bond energies, as was implied by the previously used heats of formation. The O–X stretching vibrational frequencies are known for all HOX and OX, and are reproduced in Table III. They display a monotonic decline from HOF to HOI, and from OF to OI. After taking into account the disparate masses, the corresponding force constants maintain this trend (although there is almost no change in force constant between OCl and OBr). This suggests that the HO–X bond energies might also decline monotonically from HOF to HOI, and we can see that this is not the case for HOF to HOCl. However, fluorine often introduces anomalies; cf. $D_0(F_2)$, $D_0(Cl_2)$, $D_0(Br_2)$ and $D_0(I_2)$,[28] where the bond energies decline monotonically, except between $D_0(F_2)$ and $D_0(Cl_2)$. A similar anomalous behavior between $D_0(HO-Br)$ and $D_0(HO-I)$ does not seem likely. Finally, we note that the vibrational frequencies of OX are uniformly higher than the O–X stretching frequencies in HOX. It is possible to estimate the HO–X frequencies from the O–X frequencies using Badger's rule[36] if the corresponding internuclear distances are known. In Table IV, these distances (apart from that of HO–I) are listed, and in Table III, the HO–X frequencies estimated from Badger's rule are compared with experimental values. The agreement is reasonable and enables us to predict $r(HO-I)=1.959$ Å by Badger's rule, and 1.995 Å by noting that the ratio $r(HO-X):r(O-X)$ is nearly constant.

TABLE III. The O–X stretching frequencies (in cm^{-1}) in OX[a] and HOX.[b]

OF	1053.42[c]	HOF	889.1	880[d]
OCl	853.8	HOCl	724.4	680[d]
OBr	778.7	HOBr	620.2	623[d]
OI	681.47	HOI	577/575 (matrix)	

[a]From Huber and Herzberg (Ref. 28).
[b]Summary of data given by Barnes *et al.* (Ref. 22).
[c]J. B. Burkholder, P. D. Hammer, C. J. Howard, and A. R. W. McKellar, J. Mol. Spectrosc. **118**, 471 (1986).
[d]Predicted from Badger's rule and O–X frequencies.

TABLE IV. O–X internuclear distances for OX and HOX.

X	r_e(OX) (Å)	r(O–X) in HOX (Å)	Ratio
F	1.354 12[a]	1.442[b]	0.9391
Cl	1.569 63[c]	1.6895[b]	0.9290_5
Br	1.717_2[c]	1.834[d]	0.9363
I	1.867 6[c]	(1.995) (1.959)[e]	(0.9363)

[a]See footnote c of Table III.
[b]Reference 34.
[c]Reference 27.
[d]Reference 12.
[e]From Badger's rule.

These trends in frequencies follow our suggested values for $D_0(HO-I)$ and $D_0(IO)$. With the preexisting choices for $\Delta H^0_f(HOI)$ and $\Delta H^0_f(IO)$, this pattern is not maintained.

As seen above, $D_0(IO)$ continues to be controversial after decades of study. It is not clear how difficult it will be to determine $\Delta H^0_f(HOI)$, but it has been detected mass spectrometrically,[26] and two vibrational frequencies have been reported for the gas phase.[22] However, the lifetime of HOI in the latter study was only 1–2 min. Perhaps further kinetics studies will be able to test the values suggested here. Our examination of existing studies[6] does not indicate any disparity with the currently suggested values.

With the suggested values for $\Delta H^0_f(IO)$ and $\Delta H^0_f(HOI)$, reaction (2′) (X=I) is exothermic by about 45 kcal/mol. It will be recalled that Bridier *et al.*[3] correlated the increasing rate constants of reaction (2′) with increasing exothermicity, in the sequence X=Cl, Br, I. The presently determined $\Delta H^0_f(HOBr)$, together with our surmises regarding $\Delta H^0_f(IO)$ and $\Delta H^0_f(HOI)$, now leads to the conclusion that these three reactions have approximately the same exothermicity.

B. The proton affinities of OX molecules

In Table V, we list the proton affinities of OF, OCl, and OBr at 0 and 298 K, calculated according to the available heats of formation also shown in the table. There is a large increase in proton affinity between OF and OCl, and a smaller increment between OCl and OBr. Below, we attempt to predict P.A.(OI).

TABLE V. Proton affinities of OX molecules (in kcal/mol).

X	$\Delta H_{f_0}^0$(OX)	$\Delta H_{f_0}^0$(HOX)	I.P.(HOX) (eV)	P.A.$_0$(OX)	P.A.$_{298}$(OX)
F	26±2	−19.5	12.71±0.01[a]	117.6±2	118.9±2
Cl	24.15[b]	−17.2[c]	11.12±0.01[d]	150.2	151.5
Br	31.9[b]	−10.93±0.42[e]	10.638±0.003[e]	162.7	163.9
I	(34.6)[f]	(−8 to −9)[f]	(9.71–9.80)[f]	(182–185)	(183–186)
	(41.1)[g]	(21.4±3)[g]			(202–204)[h]

[a]Reference 38.
[b]Reference 23.
[c]See footnote c of Table I.
[d]Reference 18.
[e]Present results.
[f]Suggested values (present work).
[g]Values adopted by Maguin *et al.* (Ref. 26).
[h]Based on ΔH_f^0(HOI), ΔH_f^0(IO) of Maguin *et al.* (Ref. 26), combined with I.P.(HOI) estimated above.[d]Reference 18.

Since we have already estimated $\Delta H_{f_0}^0$(OI) and $\Delta H_{f_0}^0$(HOI), we need only to estimate I.P.(HOI). If we consider OH to be a pseudohalogen, we can gain some insight by comparing the adiabatic ionization potentials of XY (Ref. 37) with XOH, where Y is a halogen atom closest in ionization potential to OH. That halogen atom is Cl. The ratio of adiabatic I.P.'s, XCl/XOH, is 1.0047, 1.0333, and 1.035 for X=F, Cl, and Br. In the case of Br, the spin–orbit splitting is 0.26 eV; the ratio to the average of the spin–orbit pair becomes 1.047. If we extrapolate this trend to X=I, the ratio is estimated to be 1.04 (1.06 to the spin–orbit average). With I.P.(ICl)=10.10 and 10.68 eV for the spin–orbit split state,[37] we infer I.P.(HOI)=9.71–9.80 eV. The proton affinity of OI deduced from these estimates is given in Table V. It is about 20 kcal/mol higher than P.A.(OBr), which is only about 12 kcal/mol higher than OCl. From the observed trends, one might anticipate a somewhat lower value for P.A.(OI). However, had we retained the prior selected values for ΔH_f^0(OI) and ΔH_f^0(HOI), combined with the currently estimated I.P.(HOI), the increment in proton affinity between OBr and OI would have been about 40 kcal/mol. Hence, the derived proton affinity of OI in Table V can be considered an additional criterion favoring the currently suggested values for ΔH_f^0(OI) and ΔH_f^0(HOI). It must also be kept in mind that our estimates began with D_0(IO)=50±5 kcal/mol; this uncertainty must be carried through the ensuing considerations.

Incidentally, one may also infer a plausible estimate for I.P.(IO), by examining the ratios of I.P.'s for XO:XOH. These ratios are 12.77 (Ref. 38)/12.71 (Ref. 39)=1.0047 and 10.87 (Ref. 40)/11.12 (Ref. 19)=0.9775 for X=F and Cl, respectively. Monks *et al.*[12] have recently determined a new I.P.(BrO)=10.46±0.02 eV, presumably supplanting the earlier value by Dunlavey *et al.*[11] 10.29±0.01 eV. The ratio of I.P.s, BrO/HOBr, is 0.9833 (Monks *et al.*) or 0.9673 (Dunlavey *et al.*). The latter maintains a monotonic trend, which suggests (but does not prove) that it may be preferred. If we extrapolate this trend, we estimate the ratio for IO/HOI to be about 0.957, which together with our earlier estimate I.P.(HOI)~9.71–9.80 eV, yields I.P.(IO)~9.29–9.38 eV. Monks *et al.*[8] had earlier rationalized their I.P.(HOBr) by comparing with the I.P.s of BrO, ClO, and HOCl. Of these four values, two come from the measurements of Monks *et al.* and a third (ClO) is given by them as 10.95±0.01 eV, but seems to be clearly 10.87±0.01 eV in the spectrum of Bulgin *et al.*[40]

C. The splitting of the first two states of HOX^+

The present results for HOBr, together with earlier studies on HOCl and HOF, enable us to construct Table VI. Here, we list the adiabatic I.P. for formation of the ground state ($X\ ^2A''$), the adiabatic value for the first excited state ($A\ ^2A'$), and their difference. These two states result from the splitting of a Π state in $C_{\infty v}$ geometry into C_s symmetry, with A'' being the out-of-plane component.

One can envisage a proton approaching OX, giving rise to this splitting. A naive view might anticipate some correlation between P.A.(OX) and the magnitude of the splitting. However, as a perusal of Tables V and VI shows, the actual behavior is contrary. The proton affinity increases as the splitting decreases.

An alternative view might attempt to correlate the splitting with the distance of the H atom (it need not and probably is not H^+) to the midpoint of the O–X bond in HOX^+. We can test such a hypothesis, with an approximation. The molecular geometries of the HOX neutral molecules except HOI are well-characterized. They will change slightly upon ionization, particularly by a diminution in the OX bond length, but for the purposes of this estimate, such a change is slight. By assuming the neutral geometries, we calculate the distance from H to the OX midpoint to be 1.274, 1.421, and 1.464 Å for HOF, HOCl, and HOBr, respectively. The shorter distance can be expected to lead to a larger splitting, as is observed.

We can extend this analysis to HOI, since we have already made estimates of its structure, i.e., r(O–H)≅0.96 Å, r(O–X)≅1.959−1.995 Å, and <HOI=102.4°. These parameters lead to r(H→OI)≅1.512−1.526 Å. The apparent de-

TABLE VI. Adiabatic values of the two lowest ionization potentials for HOX (in electron volts).

	$X\ ^2A''$	$A\ ^2A'$	$\Delta(X\ ^2A''-A\ ^2A')$	r(H→OX)
HOF	12.69±0.03[a]	14.50±0.03[a]	1.80	1.274
	12.71±0.01[b]			
HOCl	11.12±0.01[c]	12.09±0.01[c]	0.97	1.421
HOBr	10.638±0.003[d]	11.46[d]	0.82	1.464
HOI	(9.71–9.80)		(0.62–0.67)[e]	(1.512–1.526)[e]

[a]Reference 18.
[b]Reference 39.
[c]Reference 19.
[d]Present results.
[e]Estimated (see the text).

pendence of the splitting on the r(H→OX) distance is roughly exponential; the predicted splitting for HOI^+ would be ~0.62–0.67 eV.

VI. CONCLUSIONS

The adiabatic I.P. of HOBr forming the $X\ ^2A''$ state of $HOBr^+$, is found to be 10.638±0.003 eV. Autoionization structure observed is interpreted as Rydberg series converging to the first excited state $A\ ^2A'$ with an adiabatic I.P. of ~11.46 eV. The A.P. of Br^+ from HOBr is measured to be ≤13.915±0.018 eV at 0 K. This result leads directly to D_0(HO–Br)≤2.101±0.018 eV≡48.45±0.42 kcal/mol. With well-established auxiliary data, one arrives at $\Delta H^0_{f_0}$(HOBr)≥−10.93±0.42 kcal/mol, and $\Delta H^0_{f_{298}}$(HOBr)≥−13.43±0.42 kcal/mol.

With the thermochemistry of three HOX molecules rather well determined, and the fourth (HOI) poorly known, trends were examined to predict a value for ΔH^0_f(HOI)~−8 to −9 kcal/mol, much less negative than the quantity in current use (−21.4±3.0 kcal/mol).

The $X\ ^2A''$–$A\ ^2A'$ splitting in HOX^+ is found to decrease as X varies from F–Cl–Br. The proton affinity of OX is found to increase in the same order. With a plausible estimate of I.P.(HOI), the trend in proton affinity is maintained, and enables one to estimate the $X\ ^2A''$–$A\ ^2A'$ splitting in HOI^+.

The correlation of increasing rate constant with increasing exothermicity for the reactions

$$XO+HO_2\rightarrow HOX+O_2$$

as X goes from Cl–Br–I is vitiated by the current results. The exothermicity remains approximately constant.

ACKNOWLEDGMENT

This work was supported by the U.S. Department of Energy, Office of Basic Energy Sciences, under Contract No. W-31-109-Eng-38.

APPENDIX: CONVOLUTION OF KERNEL FUNCTIONS WITH THE INTERNAL DISTRIBUTION FUNCTION OF A THREE-DIMENSIONAL ROTOR

The three-dimensional rotor has the thermal distribution function

$$P(E-E_0)=\frac{2}{\sqrt{\pi}}\left(\frac{1}{kT}\right)^{3/2}(E-E_0)^{1/2}\exp[-(E-E_0)/kT],$$

where E_0 is a particular value of the photon energy $h\nu_0$. If we choose a kernel (i.e., 0 K) photoion yield curve of the form $\phi\ (E-E_t)$, then the convolution takes the following form:

(1) Prethreshold

$$I(E_0)=\int_{E_t}^{\infty}\phi(E-E_t)\,\frac{2}{\sqrt{\pi}}\left(\frac{1}{kT}\right)^{3/2}(E-E_0)^{1/2}\times\exp[-(E-E_0)/kT]dE.$$

(2) Post-threshold

$$I(E_0)=\int_0^{\infty}\phi(E-E_t)\,\frac{2}{\sqrt{\pi}}\left(\frac{1}{kT}\right)^{3/2}(E-E_0)^{1/2}\times\exp[-(E-E_0)/kT]dE.$$

1. Linear kernel function

$\phi(E-E_t)=c(E-E_t)$, where c is an arbitrary constant.

a. Prethreshold

The integral decomposes into three parts. The first has an analytical solution.

$$\frac{2ckT}{\sqrt{\pi}}\left(\frac{E_t-E_0}{kT}\right)^{3/2}e^{-(E_t-E_0)/kT}.$$

The second and third terms can be combined to give

$$\frac{2ckT}{\sqrt{\pi}}\left(\frac{3}{2}+\epsilon_0\right)\int_{\epsilon_0}^{\infty}y^{1/2}e^{-y}dy,\quad\text{where}\quad\epsilon_0=\left(\frac{E_t-E_0}{kT}\right).$$

The integral has been evaluated numerically and fitted to the following function:

$$\int_{\epsilon_0}^{\infty}y^{1/2}e^{-y}dy=e^{-\epsilon_0}\left(\frac{\sqrt{\pi}}{2}+a\epsilon_0^f\right),$$

where a=0.491 532 6, f=0.713 476 9, and the correlation is 0.999 25.

Combining all the terms, we finally obtain

$$I(E_0)=\frac{2ckT}{\sqrt{\pi}}\left(\frac{3\sqrt{\pi}}{4}+\frac{3}{2}a\epsilon_0^f-a\epsilon_0^{1+f}+\epsilon_0^{3/2}\right)e^{-\epsilon_0}.$$

b. Post-threshold

$$I(E_0)=c[\tfrac{3}{2}kT+(E_0-E_t)].$$

These two functions merge when $E_0=E_t$, at which point they both give $c(\frac{3}{2}kT)$, the average internal energy for a 3 rotor, multiplied by an arbitrary constant.

2. Exponential kernel function

$$\phi(E-E_t)=c(1-e^{-b(E-E_t)}).$$

a. Prethreshold

The integral decomposes into a b-independent part and a b-dependent part. The b-independent part has the form

$$\frac{2c}{\sqrt{\pi}}\int_{\epsilon_0}^{\infty}y^{1/2}e^{-y}dy,$$

which we have evaluated above.

Therefore, the b-independent part becomes

$$\frac{2c}{\sqrt{\pi}}\left(\frac{\sqrt{\pi}}{2}+a\epsilon_0^f\right)e^{-\epsilon_0},$$

where ϵ_0, a, and f have the same meanings as before. The b-dependent part has the form

$$J=-\frac{2c}{\sqrt{\pi}}\left(\frac{1}{kT}\right)^{3/2}\exp[-b(E_0-E_t)]\int_{E_t-E_0}^{\infty}(E_t-E_0)^{1/2}$$
$$\times\exp\left[-\left(b+\frac{1}{kT}\right)(E_t-E_0)\right]dE.$$

By analogy with the 4 rotor[41] and the requirement that the prethreshold function must match the post-threshold function at $E_t=E_0$, we assume the b-dependent part to consist of two terms—one dependent on (E_t-E_0) and the other independent (apart from the exponential $e^{-(E_t-E_0)/kT}$).

Thus, the third and fourth terms are assumed to have the form

$$-c\left(\frac{1}{bkT+1}\right)^{3/2}\exp[-(E_t-E_0)/kT]-c\left(\frac{E_t-E_0}{kT}\right)^{l}$$
$$\times\frac{1}{(bkT+1)^m}\exp[-(E_t-E_0)/kT].$$

We evaluate the integral J numerically for various values of b significantly higher and lower than the value $b=0.1$/kcal mol^{-1} previously found for CH_2OH^+.[41] After dividing J by $e^{-(E_t-E_0)/kT}$ and subtracting $(bkT+1)^{-3/2}$, the remainder is fitted numerically to a function px^l. In this manner, the energy dependence in the fourth term, i.e., l, is found to have the value 0.7, with a weak b dependence, approximately $l=-0.0325b+0.7123$. Finally, for each case of b, dividing by $[(E_t-E_0)/(kT)]^l$ exposes $(bkT+1)^{-m}$. Since $(bkT+1)$ is known, a numerical fit yields $m=0.74_4$, with good correlation. The final result is

$$I(E_0)=ce^{-\epsilon_0}\left[1+\frac{2a}{\sqrt{\pi}}\epsilon_0^f-\frac{1}{(bkT+1)^{3/2}}-\frac{\epsilon_0 l}{(bkT+1)^m}\right],$$

with a, ϵ_0, f, l, and m having the values given above.

b. Post-threshold

The convolution integral has the simple form

$$I(E_0)=c\left[1-\frac{e^{-b(E_0-E_t)}}{(bkT+1)^{3/2}}\right].$$

Thus, at $E_0=E_t$, the two functions join, with the common value

$$c[1-(bkT+1)^{-3/2}].$$

[1] Y. L. Yung, J. P. Pinto, R. T. Watson, and S. P. Sander, J. Atom. Sci. **37**, 339 (1980).
[2] G. Poulet, M. Pirre, F. Maguin, R. Ramaroson, and G. Le Bras, Geophys. Res. Lett. **19**, 2305 (1992).
[3] I. Bridier, B. Veyret, and R. Lesclaux, Chem. Phys. Lett. **201**, 563 (1993).
[4] S.-M. Fan and D. L. Jacob, Nature **359**, 522 (1992).
[5] S. W. Benson, *Thermochemical Kinetics*, 2nd ed. (Wiley, New York, 1976).
[6] R. Atkinson, D. L. Baulch, R. A. Cox, R. F. Hampson, Jr., J. A. Kerr, and J. Troe, J. Phys. Chem. Ref. Data **21**, 1125 (1992).
[7] W. B. DeMore, S. P. Sander, D. M. Golden, R. F. Hampson, M. J. Kurylo, C. J. Howard, A. R. Ravishankara, C. E. Kolb, and M. J. Molina, Evaluation Number 10, NASA JPL Publ. No. 92-20, 1992.
[8] P. S. Monks, L. J. Stief, M. Krauss, S. C. Kuo, and R. B. Klemm, J. Chem. Phys. **100**, 1902 (1994).
[9] M. P. McGrath and F. S. Rowland, J. Phys. Chem. **98**, 4773 (1994).
[10] P. S. Monks, F. L. Nesbitt, M. Scanlon, and L. J. Stief, J. Phys. Chem. **97**, 11699 (1993).
[11] S. J. Dunlavey, J. M. Dyke, and A. Morris, Chem. Phys. Lett. **53**, 382 (1978).
[12] P. S. Monks, L. J. Stief, M. Krauss, S. C. Kuo, and R. B. Klemm, Chem. Phys. Lett. **211**, 416 (1993).
[13] Y. Koga, H. Takeo, S. Kondo, M. Sugie, C. Matsumura, G. A. McRae, and E. A. Cohen, J. Mol. Spectrosc. **138**, 467 (1989).
[14] S. T. Gibson, J. P. Greene, and J. Berkowitz, J. Chem. Phys. **83**, 4319 (1985); J. Berkowitz, J. P. Greene, H. Cho, and B. Ruscic, *ibid.* **86**, 1235 (1987).
[15] G. A. McRae and E. A. Cohen, J. Mol. Spectrosc. **139**, 369 (1990).
[16] I. Schwager and A. Arkell, J. Am. Chem. Soc. **89**, 6006 (1967).
[17] S. J. Dunlavey, J. M. Dyke, and A. Morris, J. Electron. Spectrosc. **12**, 259 (1977).
[18] J. Berkowitz, J. L. Dehmer, and E. H. Appelman, Chem. Phys. Lett. **19**, 334 (1973).
[19] D. Colbourne, D. C. Frost, C. A. McDowell, and N. P. C. Westwood, J. Chem. Phys. **68**, 3574 (1978).
[20] J. Berkowitz, L. A. Curtiss, S. T. Gibson, J. P. Greene, G. L. Hillhouse, and J. A. Pople, J. Chem. Phys. **84**, 375 (1986).
[21] I. Barnes, V. Bastian, K. H. Becker, R. Overath, and T. Zhu, Int. J. Chem. Kinet. **21**, 499 (1989).
[22] I. Barnes, K. H. Becker, and J. Starcke, Chem. Phys. Lett. **196**, 578 (1992).
[23] J. L. Tech, J. Res. Natl. Bur. Stand. Ser. A **67**, 505 (1963); R. E. Huffman, J. C. Larrabee, and Y. Tanaka, J. Chem. Phys. **47**, 856 (1967).
[24] L. V. Gurvich, I. V. Veyts, and C. B. Alcock, *Thermodynamic Properties of Individual Substances* (Hemisphere, New York, 1989); *ibid.* (Hemisphere, New York, 1991), Vol. 2.
[25] R. B. Boodaghians, I. W. Hall, and R. P. Wayne, J. Chem. Soc. Faraday Trans. 2 **83**, 529 (1987).
[26] F. Maguin, G. Laverdet, G. LeBras, and G. Poulet, J. Phys. Chem. **96**, 1775 (1992).
[27] M. E. Jenkin, K. C. Clemitshaw, and R. A. Cox, J. Chem. Soc. Far. Trans. 2 **80**, 1633 (1984).
[28] K. P. Huber and G. Herzberg, *Molecular Spectra and Molecular Structure* (Van Nostrand, New York, 1979), Vol. 4.
[29] A. G. Gaydon, *Dissociation Energies*, 3rd ed. (Chapman and Hall, London, 1968).
[30] D. St. A. G. Radlein, J. C. Whitehead, and R. Grice, Nature **253**, 37 (1975); Mol. Phys. **29**, 1813 (1975).
[31] R. R. Reddy, T. V. R. Rao, and A. S. R. Reddy, Indian J. Pure Appl. Phys. **27**, 243 (1989).
[32] J. Garraway and R. J. Donovan, J. Chem. Soc. Chem. Commun. **1979**, 1108.
[33] W. F. Schneider, T. J. Wallington, M. D. Harley, J. Schested, and O. J. Nielsen, J. Phys. Chem. **98**, 2217 (1994).
[34] S. W. Benson, J. Phys. Chem. **98**, 2216 (1984).
[35] H. H. Landolt and R. Börnstein, *Structure Data of Free Polyatomic Molecules*, edited by K.-H. Hellwege (Springer, Berlin, 1976), Vol. 7, pp. 42, 60.
[36] G. Herzberg, *Molecular Spectra and Molecular Structure* (Van Nostrand, Princeton, NJ, 1950), Vol. 1, p. 457.
[37] J. M. Dyke, G. D. Josland, J. G. Snijders, and P. M. Boerrigter, Chem. Phys. **91**, 419 (1984).
[38] J. M. Dyke, N. Jonathan, J. D. Mills, and A. Morris, Mol. Phys. **40**, 1177 (1980).
[39] J. Berkowitz, E. H. Appelman, and W. A. Chupka, J. Chem. Phys. **58**, 1950 (1973).
[40] D. K. Bulgin, J. M. Dyke, N. Jonathan, and A. Morris, Mol. Phys. **32**, 1487 (1976).
[41] B. Ruscic and J. Berkowitz, J. Phys. Chem. **97**, 11451 (1993).